

Linking *P-T* path with development of discontinuous phosphorus zoning in garnet during high-temperature metamorphism – an example from Lützow-Holm Complex, East Antarctica

Tetsuo KAWAKAMI* and Tomokazu HOKADA***

**Department of Geology and Mineralogy, Graduate School of Science,
Kyoto University, Kyoto 606-8502, Japan*

***National Institute of Polar Research, 10-3 Midori-cho, Tachikawa, Tokyo 190-8518, Japan*

****Department of Polar Science, The Graduate University for Advanced Studies,
10-3 Midori-cho, Tachikawa, Tokyo 190-8518, Japan*

Garnet porphyroblasts contained in the garnet-sillimanite gneiss from the Lützow-Holm Complex at Skalklevikshalsen, East Antarctica, have a phosphorus-poor core and phosphorus-rich rim. The core/rim boundary of the phosphorus zoning is discontinuous. The irregular shape of this core/rim boundary together with the pressure difference between the core and the rim inferred from the difference in aluminosilicate inclusions (kyanite in the core and sillimanite in the rim) suggests that this is the resorption/precipitation boundary. The difference between phosphorus concentrations in the garnet core and rim is accompanied by a change in phosphate inclusions in the garnet. Apatite and monazite are included in the phosphorus-poor garnet core, whereas monazite alone is included in the phosphorus-rich garnet rim. Utilizing the core/rim boundary as a contemporaneous surface when comparing different garnet grains, the timing of the discontinuous phosphorus-zoning formation (and thus, the garnet resorption) and change in the phosphate assemblage can be correlated to the pressure-temperature path of the garnet-sillimanite gneiss. The phosphorus-poor core of the garnet mainly formed during the prograde stage in the kyanite to sillimanite stability fields under which apatite probably buffered the phosphorus-content of garnet, and the phosphorus-rich garnet rim possibly crystallized from the melt at the retrograde stage near the vapor saturated solidus under which monazite alone (without apatite) probably did not buffer the phosphorus-content of garnet. Garnet resorption occurred during the decompression stage between these two garnet growth stages.

Keywords: Apatite, Garnet, Buffer, Partial melting, Phosphorus

INTRODUCTION

In high-temperature metamorphic rocks, chemical zoning of garnet in terms of major elements such as Ca, Fe, Mg, and Mn is often obscured by the diffusion under high-temperature conditions (e.g., Hiroi et al., 1995). However, it is well known that some minor elements like phosphorus commonly preserve chemical zoning with a non-diffusive nature even in the high-temperature metamorphic rocks (Hiroi and Ellis, 1994; Spear and Kohn, 1996; Hiroi, 1997; Hiroi et al., 1997; Chernoff and Carlson, 1999; Yang and Rivers, 2002; Yoshimura et al., 2004). Their zoning pattern is best observed under X-ray elemental

mapping and it is characterized by a drastic, discontinuous change in their concentration within garnet (for examples of such zoning, see Hiroi et al., 1997; Chernoff and Carlson, 1999; Yang and Rivers, 2002; Yoshimura et al., 2004; Kawakami et al., 2008). Zoning in minor elements that is not affected by the diffusion in garnet is important because it can represent the contemporaneous surface (cf., Chernoff and Carlson, 1999) and contain considerable information about the reaction history that the rock has experienced (Spear and Pyle, 2002) even if the major element zoning in garnet is obscured by the later diffusion.

In order to elicit such information and to understand their formation mechanism, it is convenient to utilize relict mineral inclusions preserved in garnet. Minerals like aluminosilicates are useful in constraining the *P-T* path,

doi:10.2465/jmps.080501a

T. Kawakami, t-kawakami@kueps.kyoto-u.ac.jp Corresponding author

and zircon, monazite, and apatite inclusions may constrain the age of garnet growth. Therefore, the pressure-temperature-time (P - T - t) path can be potentially correlated with the event that formed the chemical zoning of minor elements in garnet, and finally, with the duration and rate of tectono-metamorphism (Kelsey et al., 2008). Furthermore, if the formation mechanism of the minor element zoning can be correlated with the presence or absence of melt, we can constrain the change in the physical properties of the metamorphic rocks in the deep crust as a function of their P - T - t evolution.

Discontinuous, stepwise chemical zoning of phosphorus that is often preserved in garnet from the high-temperature metamorphic rocks has been considered to have formed through partial melting (Hiroi et al., 1997). Hiroi (1997) concluded that the stepwise increase in phosphorus in the garnet rim was attributable to the change from the phosphate-undersaturated condition under which the garnet core grew in the presence of melt and the absence of phosphates to the phosphate-saturated condition under which the garnet rim grew during the melt crystallization in the presence of phosphates. However, our example is different from the case of Hiroi (1997) because phosphates are included in both the core and the rim. Therefore, there should exist some different aspects in the mechanism of discontinuous, stepwise phosphorus-zoning formation.

In this study, the systematic correlation between the change in the phosphate assemblage and phosphorus zoning in garnet that is observed in the garnet-sillimanite gneiss from the Lützow-Holm Complex at Skallevikshalsen, East Antarctica, is described, and the formation mechanism of phosphorus zoning of garnet in the studied sample, especially the possible occurrence of the phosphorus-buffer reaction, is discussed.

GEOLOGY OF LÜTZOW-HOLM COMPLEX (LHC) AT SKALLEVIKSHALSEN

The LHC is a Cambrian orogenic belt bounded by the Late Proterozoic to Cambrian Rayner Complex to the east and by the Late Proterozoic to Early Palaeozoic Yamato-Belgica Complex to the west (Shiraishi et al., 1992, 1994, 2003) (Fig. 1). For a detailed summary of the surrounding Complexes, see Satish-Kumar et al. (2008). The LHC is composed of high-grade metamorphic rocks such as mainly pelitic-psammitic gneisses and mafic to intermediate gneisses, along with a subordinate amount of ultramafic lenses, marble, and calc-silicate rocks. Felsic pegmatitic dykes discordantly intrude into these metamorphic rocks. The metamorphic grade of the complex progressively changes from upper amphibolite facies on the Prince Olav Coast to granulite facies in the Lützow-Holm Bay (Hiroi et al., 1991) (Fig. 1). A “thermal axis” of the

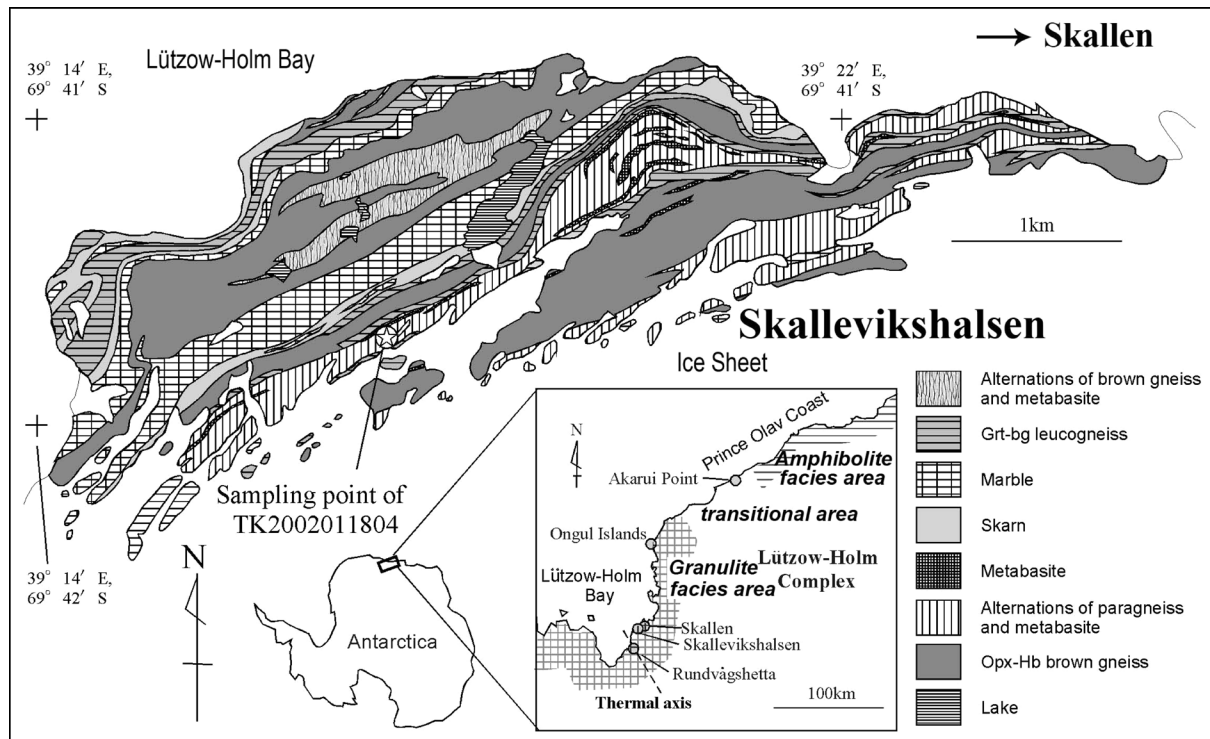


Figure 1. Simplified metamorphic zone map of the Lützow-Holm Complex (after Hiroi et al., 1991) and the geological map of Skallevikshalsen showing the sample locality (after Yoshida et al., 1976).

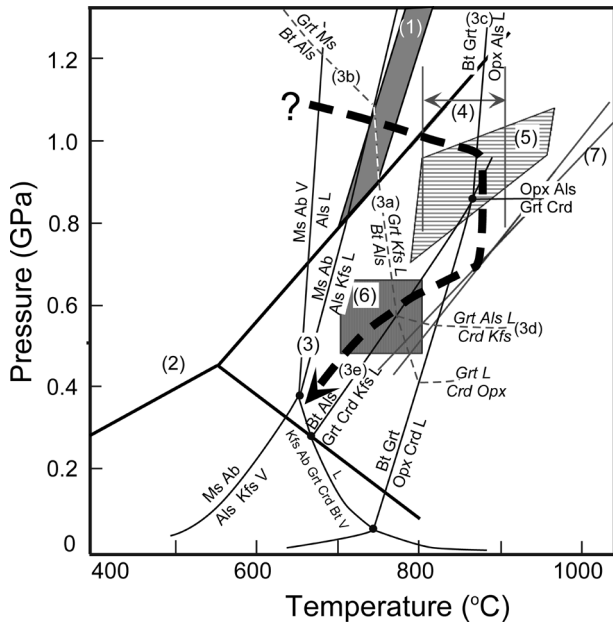


Figure 2. Summary of the *P-T* conditions estimated by previous studies and inferred *P-T* path (thick broken line and arrow, respectively) of the Skallevikshalsen rocks (after Kawakami and Motoyoshi, 2004; Satish-Kumar et al., 2006). The *P-T* estimates for adjacent Skallen areas (several kilometers away from Skallevikshalsen) are also shown. The *P-T* estimates and reaction lines shown in Figure 2 are as follows. (1) Reaction line of staurolite = garnet + kyanite + hercynite + H₂O (dark grey area; Hiroi et al., 1994). (2) Aluminosilicate diagram of Pattison (1992), indicated by a thick solid line. (3) Melting reaction curves in the NaKFMASH system (thin solid lines and thin dotted lines) cited from Spear et al. (1999). Thin dotted lines with italic mineral abbreviations indicate contours of $X_{Fe} = 0.70$ in garnet for selected divariant assemblages. Quartz and albite are excess phases. See the text for a detailed explanation of reactions 3a–3e. Note that the value of X_{Fe} for the whole-rock garnet-sillimanite gneiss is 0.70, and that for the garnet is 0.67–0.70 (Kawakami and Motoyoshi, 2004). (4) Peak metamorphic temperature of 848 ± 55 °C from Skallen (arrow; Satish-Kumar and Wada, 2000). (5) Peak *P-T* estimate from Skallevikshalsen (lateral striped area; Yoshimura et al., 2004). (6) Retrograde *P-T* estimate from Skallen (light grey plaid area; Ikeda, 2004). (7) Reaction line of garnet + sillimanite = spinel + quartz with the effect of ZnO in spinel being considered (grey lines; Kawakami and Motoyoshi, 2004).

maximum peak temperature is estimated to lie at the southern Lützow-Holm Bay, around Rundvågshetta (Motoyoshi, 1986). Ultrahigh-temperature (*UHT*) metamorphism at approximately 1000 °C and 1.1 GPa, and subsequent isothermal decompression are reported from Rundvågshetta (Kawasaki et al., 1993; Ishikawa et al., 1994; Motoyoshi and Ishikawa, 1997). In addition to the orthopyroxene + sillimanite ± quartz assemblage in the rock matrix (Motoyoshi and Ishikawa, 1997), the sapphirine + quartz assemblage is also found as an inclusion in garnet (Yoshimura et al., 2008) to indicate the *UHT* condition in Rundvågshetta. The complex is deduced to have

experienced a typical “clockwise” *P-T* path (Fig. 2), evidenced by the presence of prograde kyanite and staurolite as relict inclusions in garnet or plagioclase (Hiroi et al., 1983a, 1983b; Motoyoshi, 1986; Kawakami and Motoyoshi, 2004; Satish-Kumar et al., 2006) and by the reaction textures in ultramafic rocks (Hiroi et al., 1986). The rocks in the Prince Olav Coast experienced the reaction staurolite = garnet + aluminosilicate + spinel + H₂O in the sillimanite stability field whereas those in the Lützow-Holm Bay experienced the reaction in the kyanite stability field (reaction 1 in Fig. 2, Hiroi et al., 1983a, 1983b, 1991). The progressive change in the metamorphic grade from the upper amphibolite facies to the *UHT* condition led previous researchers to use this complex when comparing the differences between metamorphic evolution in the high-temperature and the *UHT* regions found in the same complex (e.g., Kawakami et al., 2006).

Skallevikshalsen lies on the eastern coast of the Lützow-Holm Bay, approximately 30 km northeast of Rundvågshetta (Fig. 1). Skallevikshalsen is underlain by well-layered metamorphic rocks including orthopyroxene-hornblende brown gneiss, garnet-bearing felsic gneisses (garnet-biotite gneiss and garnet-sillimanite gneiss), marble, skarn, metamafic rocks including garnet-two pyroxene gneiss, and subordinate amounts of granitic pegmatites (Fig. 1). Orthopyroxene-hornblende brown gneiss is the most common lithology. The garnet-two pyroxene gneiss is commonly boudinaged, and leucosome is developed at the interboudin partitions between and within the granulite lens, indicating the occurrence of partial melting. All lithologies except granitic pegmatites are strongly deformed. At least two timings of deformation can be recognized from the fold interference patterns; an isoclinal fold with the fold axis trending NE-SW and the axial plane almost parallel to the chemical banding of surrounding rocks, and a tight to open fold with the fold axis trending NE-SW and a steeply dipping axial plane (Kawakami and Ikeda, 2004). The garnet-sillimanite gneiss is intercalated with metamafic rocks and locally contains lenses of garnet-two pyroxene gneiss.

Using several geothermometers and geobarometers, Yoshimura et al. (2004) estimated the peak metamorphic conditions of Skallevikshalsen to be 770–940 °C and 0.65–1.2 GPa for the garnet-biotite gneiss, and 780–960 °C and 0.60–1.1 GPa for the garnet-two pyroxene gneiss (Fig. 2). Based on the *P-T* conditions that permit partial melting of the typical pelitic rocks, migmatitic appearance of the garnet-biotite gneiss, and occurrence of euhedral feldspar and quartz inclusions in the garnets in them, they concluded that this lithology experienced partial melting. They also considered that partial melting also occurred in the garnet-sillimanite gneiss and this rock type is likely to

be the restitic product of partial melting based on the BaO content in K-feldspar and P_2O_5 and Y_2O_3 contents in garnet (Yoshimura et al., 2004). Dunkley (2007) carried out U-Pb SHRIMP dating of zircon from Skallevikshalsen, and reported spread ages of 630–500 Ma.

ANALYTICAL METHODS

The X-ray mapping of the garnet grains were obtained using a JEOL JXA8800M at the National Institute of Polar Research (NIPR); JEOL JXA-8800R superprobe at the Institute of Geology and Geoinformation, National Institute of Advanced Industrial Science and Technology (AIST); and JEOL JXA-8105 superprobe at Kyoto University. The analytical conditions for X-ray mapping were an acceleration voltage of 15.0 kV and a probe current of 400–800 nA with a focused beam to defocused beam having a diameter of up to 5 μm . Inclusion minerals were identified using a Hitachi S3500H scanning electron microscope equipped with EDAX X-ray analytical system at Kyoto University. Aluminosilicates were identified by Raman spectroscopy at NIPR (JASCO NRS 1000) and Kyoto University (JASCO NRS 3100). Minerals were quantitatively analyzed using a JEOL JXA-8105 superprobe at Kyoto University. The analytical conditions were an acceleration voltage of 15.0 kV and a probe current of 10 nA with a probe diameter of 3 μm . The counting time for the peak and backgrounds were 30 s and 15 s for phosphorus and yttrium, respectively, and 10 s and 5 s for

other elements. Natural and synthetic minerals were used as standards, and ZAF correction was applied. The detection limit for P_2O_5 was approximately 160 ppm (1σ level).

SAMPLE DESCRIPTION

The sample used in this study (sample No. TK2002011804) is a garnet-sillimanite gneiss that mainly consists of garnet (diameter: approximately 5 mm), sillimanite, K-feldspar, plagioclase, and quartz with minor amounts of zircon and monazite. The rock matrix contains no hydrous mineral except for local retrograde biotite. Apatite is very rare in the rock matrix. XRF analyses suggests that the sample contains 0.07 wt% whole-rock P_2O_5 (Kawakami and Motoyoshi, 2004). This sample is the same lithology as the garnet-sillimanite gneiss studied by Yoshimura et al. (2004).

Garnet grains from one hand specimen were used in this study because the use of different hand specimens may cause a variation in the whole-rock composition, difference in the mineral assemblage, and difference in the modal amount of minerals contained in it. This variation may affect the behavior of phosphates and phosphorus during metamorphism, making it difficult to compare the timing of phosphorus-zoning formation in different garnet grains. Using samples from the same hand specimen minimizes such an effect.

The garnet-sillimanite gneiss used in this study affords an advantage for estimating the P - T path in that it

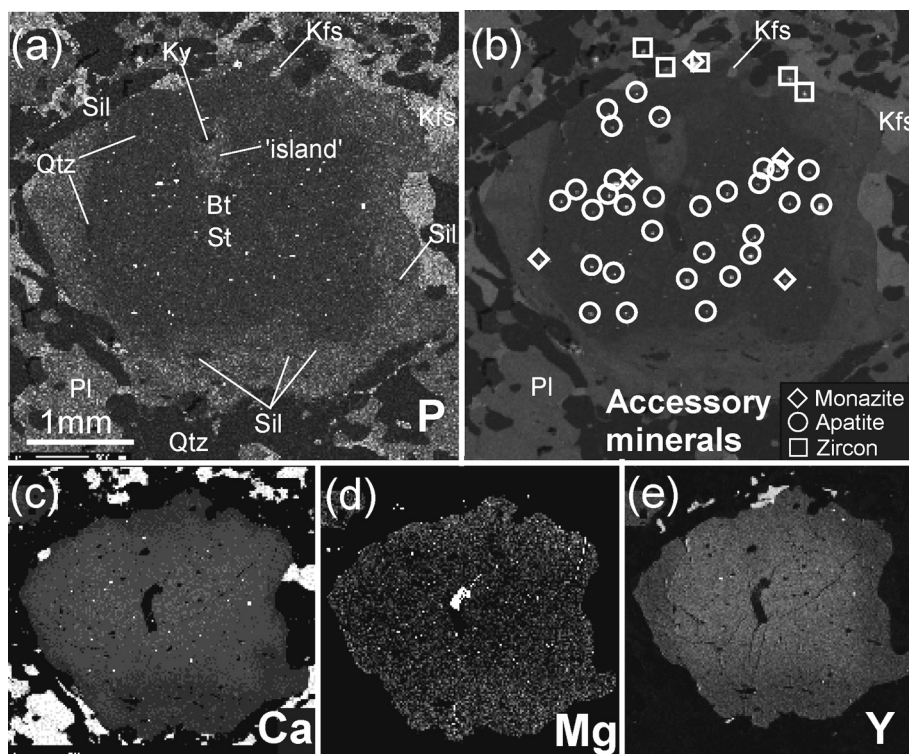


Figure 3. (a) and (b) X-ray elemental maps of garnet A in terms of phosphorus, showing the distribution of major inclusion minerals and accessory minerals (apatite, monazite, and zircon). The core includes staurolite, biotite, quartz, apatite, monazite (up to 24 μm , the size of monazite is that of the long axis hereafter), and fine-grained zircon, whereas the rim includes sillimanite needles and coarse-grained zircon. Note the difference in accessory phases present in the garnet core and in the rim and the rock matrix. No phosphate is included in the phosphorus-rich rim. Coarse-grained zircon and coarse-grained monazite (53 μm) are present in the rock matrix next to garnet. K-feldspar is included at the boundary of the core and rim. The phosphorus-poor core in this garnet grain has a patchy phosphorus-rich “island” in which kyanite is included. (c) X-ray elemental map of Ca. (d) X-ray elemental map of Mg. (e) X-ray elemental map of Y. Y content is high in the core.

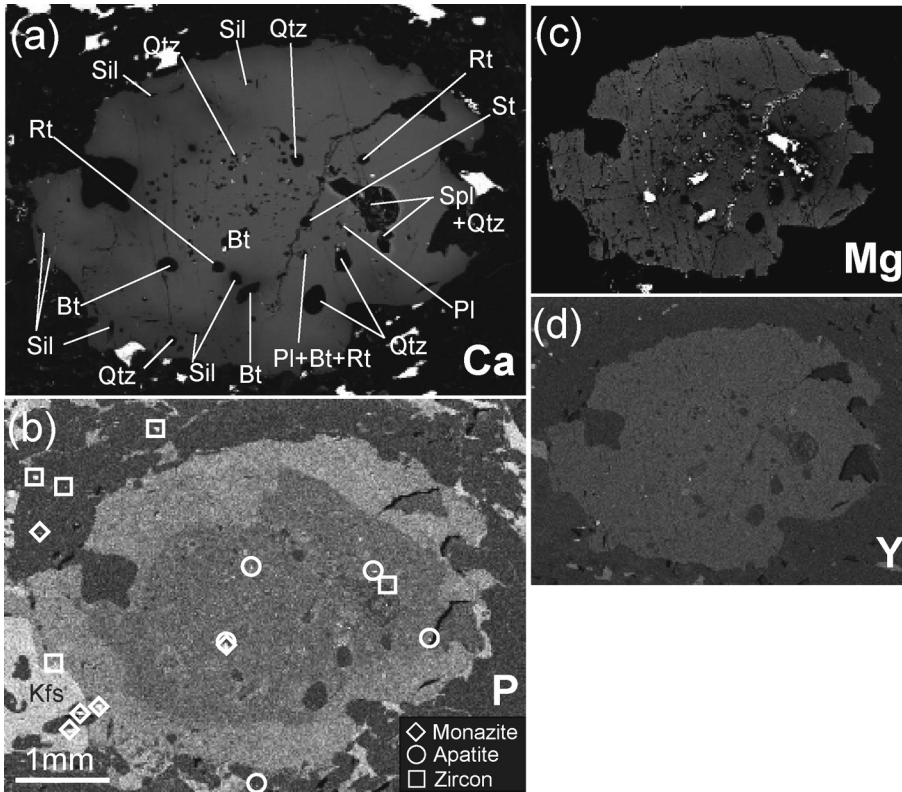


Figure 4. (a) and (b) X-ray elemental maps of garnet B in terms of Ca and phosphorus. The core includes staurolite, biotite, quartz, rutile, spinel + quartz + biotite, albitic plagioclase + biotite + rutile, prismatic sillimanite, apatite, fine-grained monazite (up to 37 μm), and fine-grained zircon, whereas the rim includes sillimanite needles, quartz, and coarse-grained monazite (59 μm). Coarse-grained monazite (105 μm) is also present in the rock matrix. The inconsistency between sharp phosphorus-zoning and gradual major element zoning is particularly clear around the coarse-grained prismatic sillimanite inclusion where an embayment of a Ca-poor part is developed continuously from the rim. (c) X-ray elemental map of Mg. (d) X-ray elemental map of Y.

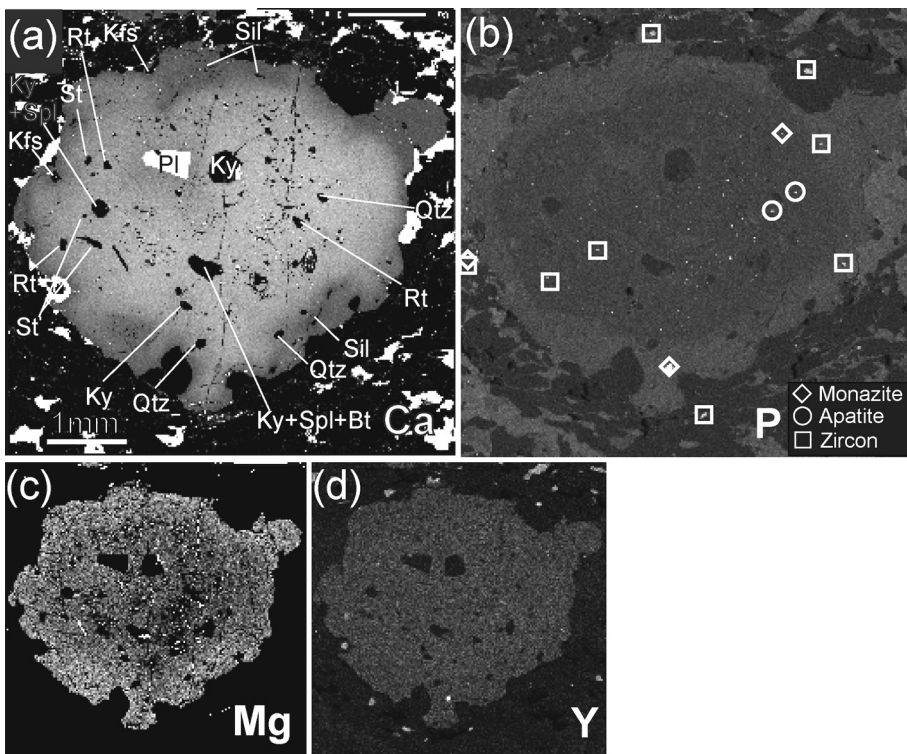


Figure 5. (a) and (b) X-ray elemental maps of garnet C in terms of Ca and phosphorus. The core includes kyanite, plagioclase, rutile, multi-phase inclusion of kyanite + spinel + biotite (possibly after staurolite), staurolite, quartz, apatite, fine-grained monazite, and fine-grained zircon. The rim includes sillimanite needles, K-feldspar, quartz, and coarse-grained monazite (103 μm) and zircon. In the rock matrix near the garnet, coarse-grained zircon grains occur. (c) X-ray elemental map of Mg. (d) X-ray elemental map of Y. No Y zoning is recognized in this grain.

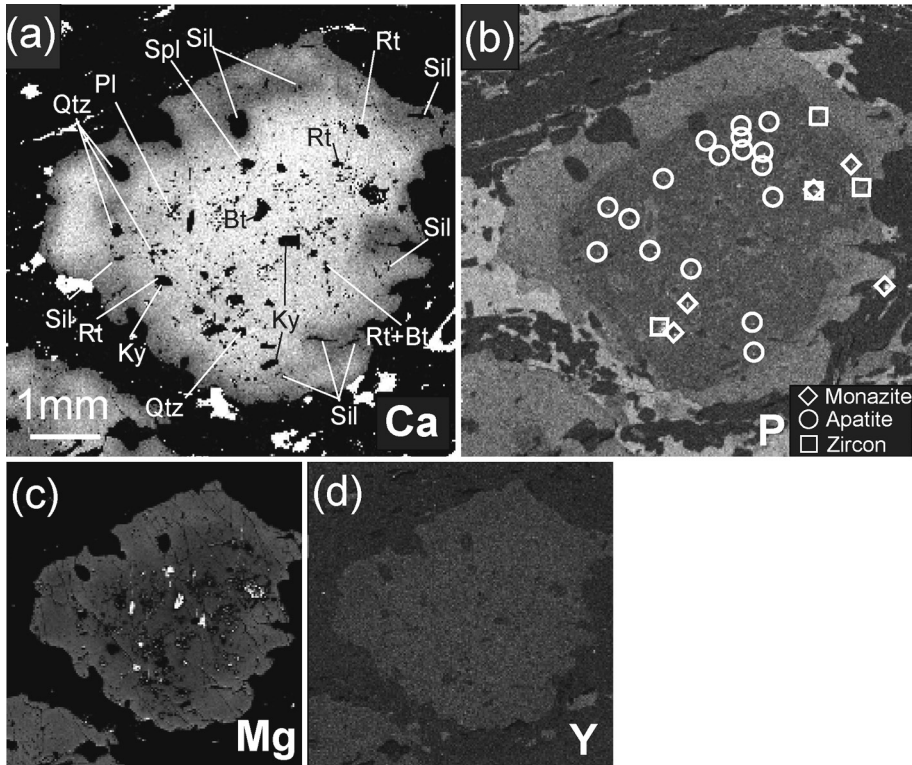


Figure 6. (a) and (b) X-ray elemental maps of garnet D in terms of Ca and phosphorus. The garnet core includes biotite, plagioclase, quartz, rutile, spinel, kyanite, prismatic sillimanite, apatite, fine-grained zircon, and coarse-grained monazite. The rim includes sillimanite needles and quartz. Locally, a sillimanite needle is included at the boundary between the core and the rim, cutting the sharp phosphorus zoning. Coarse-grained monazite occurs in the rock matrix near the garnet. The Ca concentration is low at the garnet rim where sillimanite is included. (c) X-ray elemental map of Mg. The Mg-content is higher in the rim. (d) X-ray elemental map of Y. Y content is slightly high in the core.

includes many relic inclusions in the garnet porphyroblasts (Figs. 3–7). The garnet grains have sharp zoning in phosphorus, and the core and rim parts of the garnet are defined using the zoning in phosphorus, that is, phosphorus-poor core and phosphorus-rich rim. The garnet core includes biotite, staurolite, kyanite, kyanite + spinel + biotite association (possibly after staurolite), prismatic sillimanite, spinel + quartz association, plagioclase, quartz, rutile, fine-grained zircon, apatite, and fine-grained monazite (up to 52 μm), whereas the rim includes sillimanite needles, plagioclase, K-feldspar, quartz, coarse-grained zircon, and coarse-grained monazite (up to 147 μm). K-feldspar is included in the rim or at the boundary between the core and the rim (Figs. 3 and 5). Prismatic sillimanite in the core (Fig. 4) is rare; however, it is found in the garnet grain that includes spinel + quartz assemblage. This grain only exhibits the outermost core part and the rim because the thin section is off the center of this garnet grain. Some garnet cores have a patchy phosphorus-rich “island” in which kyanite (Fig. 3) or an aggregate of muscovite + quartz + chlorite (Fig. 7f) are included.

As described above, the phosphorus-poor core includes two types of phosphates, i.e., apatite and monazite, although the phosphorus-rich rim includes only monazite. The enlargement of the core/rim boundary represented by the elemental mapping of phosphorus is shown in Figure 7c. As is evident from this map, the rim part is not homogeneous in terms of phosphorus concentration, and in-

stead exhibits oscillatory-like zoning. The P_2O_5 concentration of the phosphorus-rich rim and “island” ranges from below the detection limit up to 1040 ppm (312 ppm on average). On the other hand, most of the core is below the detection limit of phosphorus, except for the local high-phosphorus patches. Representative analyses of garnet are listed in Table 1.

The core of the garnet is commonly Cr-poor and Y-rich, and the rim is Cr-rich and Y-poor (e.g., Fig. 3). In some garnet grains, zoning in Y is very weak and difficult to identify (e.g., Fig. 4). Weak zoning in Cr and Y are, if present, correlated with phosphorus zoning although the core/rim boundary is not as sharp as that of phosphorus. Chemical zoning in terms of Ca, Mg (e.g., Fig. 3), and Fe are gradual and locally oblique to the chemical zoning by phosphorus. The Ca concentration is low at the garnet rim where sillimanite needles are included.

DISCUSSION

Interpretation of chemical zoning preserved in studied garnet

The phosphorus zoning of garnet is discontinuous and sharp, and therefore, it is almost unaffected by the diffusion. This is probably because the incorporation of phosphorus into garnet is the coupling substitution likely to be $2\text{Si} = \text{AlP}$, and thus, the intracrystal diffusion of phospho-

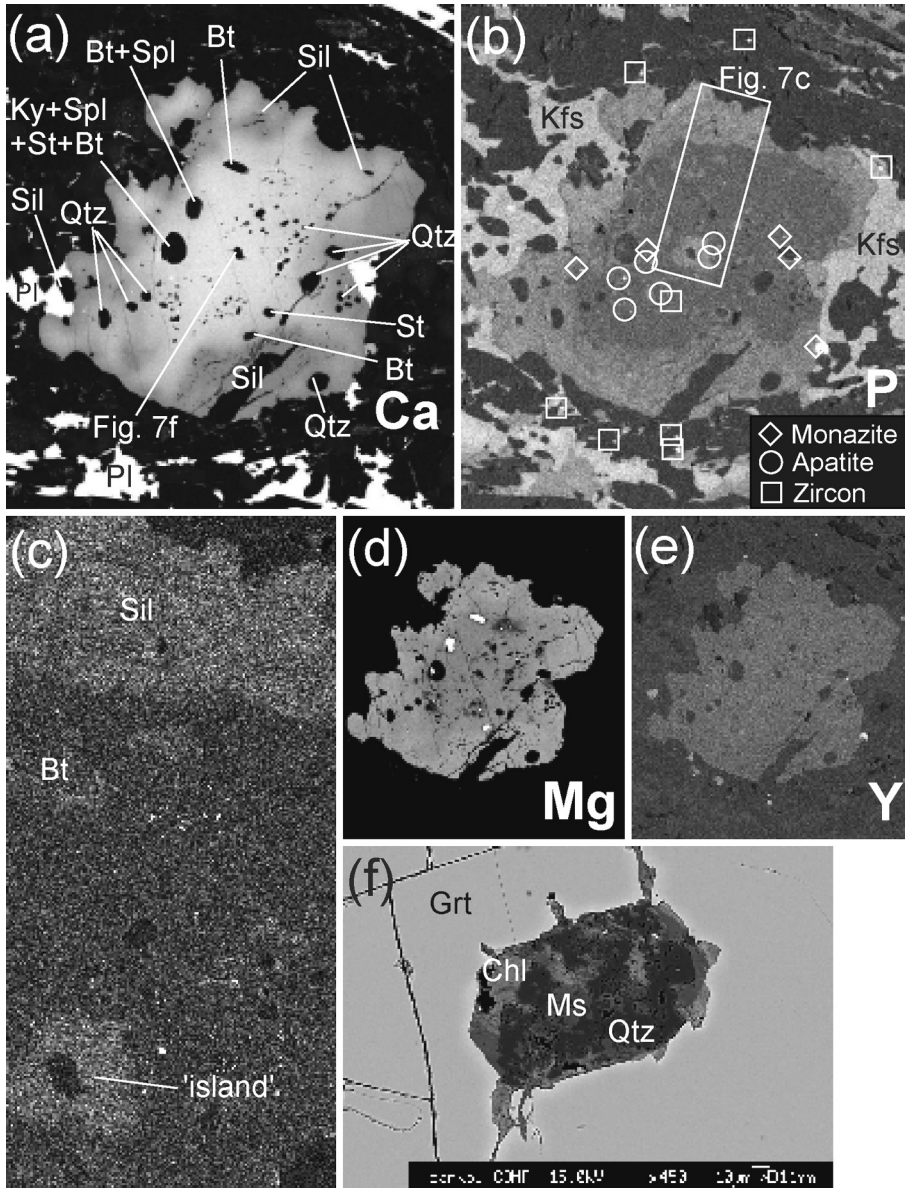


Figure 7. (a) and (b) X-ray elemental maps of garnet E in terms of Ca and phosphorus. The garnet includes an aggregate of kyanite + spinel + biotite + staurolite (Fig. 2d of Kawakami and Motoyoshi, 2004), staurolite, biotite, quartz, muscovite + quartz intergrowth, fine-grained monazite (up to 52 μm), apatite, and zircon. The rim includes sillimanite needles and quartz. Coarser-grained monazite (147 μm) and zircon than those included in the garnet are present in the matrix near the garnet. The phosphorus-rich “island” including muscovite + quartz intergrowth is present in the core of this garnet. (c) Enlargement of the boxed part of Figure 7b. Note the oscillatory-like zoning of phosphorus in the garnet rim. (d) X-ray elemental map of Mg. (e) X-ray elemental map of Y. Y content is slightly high in the core. (f) Back-scattered electron image of faceted inclusion of muscovite + quartz (+ chlorite) intergrowth included in the phosphorus-rich “island.” Chlorite is developed along cracks radiating from the inclusion and also between the garnet and the muscovite + quartz intergrowth. Therefore, it is likely a retrograde reaction product between the garnet and the inclusion.

rus is sluggish (London, 1997). Because the studied garnet grains are from the same hand specimen, the core/rim boundary defined by the discontinuous, stepwise phosphorus zoning is not largely controlled by the variation in local whole-rock composition. Rather, a systematic change in the phosphate inclusions in garnet and correlation with phosphorus zoning suggest that the phosphorus zoning can be attributed to a phosphate-bearing reaction and that it represents the contemporaneous surface, at least within the hand specimen scale (cf., Chernoff and Carlson, 1999).

On the other hand, chemical zoning of the garnet in terms of Ca, Mg, and Fe do not preserve the idiomorphic shape of garnet and are not even concordant with the zoning by phosphorus. Therefore, it is apparent that zoning in major elements does not record information about the

prograde stage when the garnet core grew. It is strongly affected by the diffusion during high-temperature metamorphism. Taking into account the fact that the concentration of Ca is concordant with the distribution of sillimanite inclusions in the garnet core and rim (Figs. 3–7), the Ca zoning has been likely modified during the retrograde stage, recording information after garnet rim formation in the sillimanite stability field.

The shape of the core/rim boundary defined by the sharp phosphorus zoning reported from the garnet-sillimanite gneiss is generally irregularly shaped and not euhedral (e.g., Hiroi et al., 1997; Yoshimura et al., 2004). Furthermore, the formation conditions of the phosphorus-rich rim and the phosphorus-poor core differ considerably, especially in terms of the pressure condition, as suggested from the different aluminosilicate inclusions.

Table 1. Representative analyses of garnet in sample TK2002011804

Sample	011804c	011804c	011804c	011804c
	Grt core	Grt core	Grt island	Grt rim
Analyses number	081021ka	081021ka	081014ka	081021ka
	wa01-11	wa01-9	wa01-3	wa01-5
SiO ₂	39.32	39.15	39.62	39.18
Al ₂ O ₃	22.51	22.60	22.56	22.20
Cr ₂ O ₃	0.01	n.d.	0.04	0.07
FeO	28.86	29.52	28.96	30.46
MnO	0.35	0.34	0.36	0.38
MgO	8.57	8.35	8.30	8.38
CaO	1.47	1.55	1.85	1.11
P ₂ O ₅	n.d.	0.03	0.11	0.07
Y ₂ O ₃	0.03	0.01	0.08	n.d.
Total (wt%)	101.1	101.5	101.8	101.8
Number of O	12	12	12	12
Si	3.002	2.986	3.007	2.991
Al	2.025	2.031	2.017	1.997
Cr	0.001	n.d.	0.003	0.004
Fe	1.842	1.882	1.838	1.944
Mn	0.022	0.022	0.023	0.025
Mg	0.974	0.949	0.938	0.953
Ca	0.120	0.126	0.150	0.091
P	n.d.	0.001	0.003	0.002
Y	0.001	0.001	0.004	n.d.
Total cation	7.986	7.998	7.983	8.009
Mg/(Fe+Mg)	0.35	0.34	0.34	0.33

n.d., not detected.

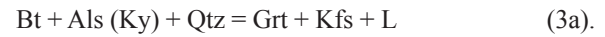
Therefore, in the garnet-sillimanite gneiss from Skallevikshalsen, garnet was partially resorped between the core-formation stage and the rim formation stage. The irregularly shaped core/rim boundary defined by the discontinuous phosphorus zoning represents the resorption/precipitation boundary of the garnet.

Timing of discontinuous phosphorus-zoning formation in garnet - correlation with *P-T* path

In this section, we discuss the timing of discontinuous phosphorus-zoning formation correlated with the *P-T* path. In particular, the reaction sequence is explained in detail because it is important to constrain the timing of garnet growth during the *P-T* evolution in order to understand the formation mechanism of phosphorus zoning. Figure 8 illustrates the textural development of the garnet.

The presence of biotite as an inclusion in the garnet core indicates that the garnet-sillimanite gneiss originally contained biotite in the matrix during prograde metamorphism. The presence of kyanite and staurolite inclusions in the garnet core suggests that garnet core growth occurred under the kyanite stability field. Yoshimura et al. (2004) implied that partial melting of biotite-bearing felsic gneiss in Skallevikshalsen occurred during high-*T*

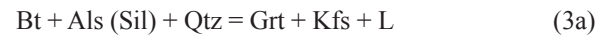
metamorphism. Combining this information suggests that the reaction for the garnet core growth is presumably a continuous reaction:



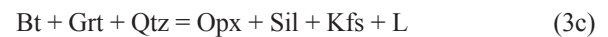
The bracketed numbers following the reaction equations such as (3a) correspond to the numbers for the reaction lines shown in Figures 2 and 8. Because muscovite is not commonly found as an inclusion in garnet, the reaction:



is not likely to be responsible for the garnet growth (Figs. 2 and 8). Sillimanite inclusions in the outermost core of the garnet suggest that the continuous reaction:



also occurred in the sillimanite stability field (Fig. 8). It is likely that the attainment of the peak metamorphic condition determined by Yoshimura et al. (2004) followed by crossing or not crossing the NaKFMASH univariant reaction (in the presence of albite):



although the whole-rock composition of the garnet-sillimanite gneiss (more Fe-rich than the Als-Grt tie line) only permitted the assemblage of Grt + Sil + Kfs + L, which is concordant with the matrix mineral assemblage presently observed in the garnet-sillimanite gneiss. After the attainment of the peak metamorphic condition, the rock probably experienced decompression and crossed the reaction:



to produce Spl + Qtz (Kawakami and Motoyoshi, 2004). Incomplete back reaction of this reaction could form an inclusion of this assemblage in the garnet outermost core (Fig. 8). Further decompression with temperature decrease possibly occurred above the reaction line:



for $X_{\text{Fe}}^{\text{Grt}} = 0.70$ so that cordierite was not formed, because the X_{Fe} value of the whole-rock sample is 0.70 (Kawakami and Motoyoshi, 2004) and that of the garnet is similar ($X_{\text{Fe}}^{\text{Grt}} = 0.67-0.70$). After entering the *P-T* field above the NaKFMASH univariant reaction (in the presence of albite):

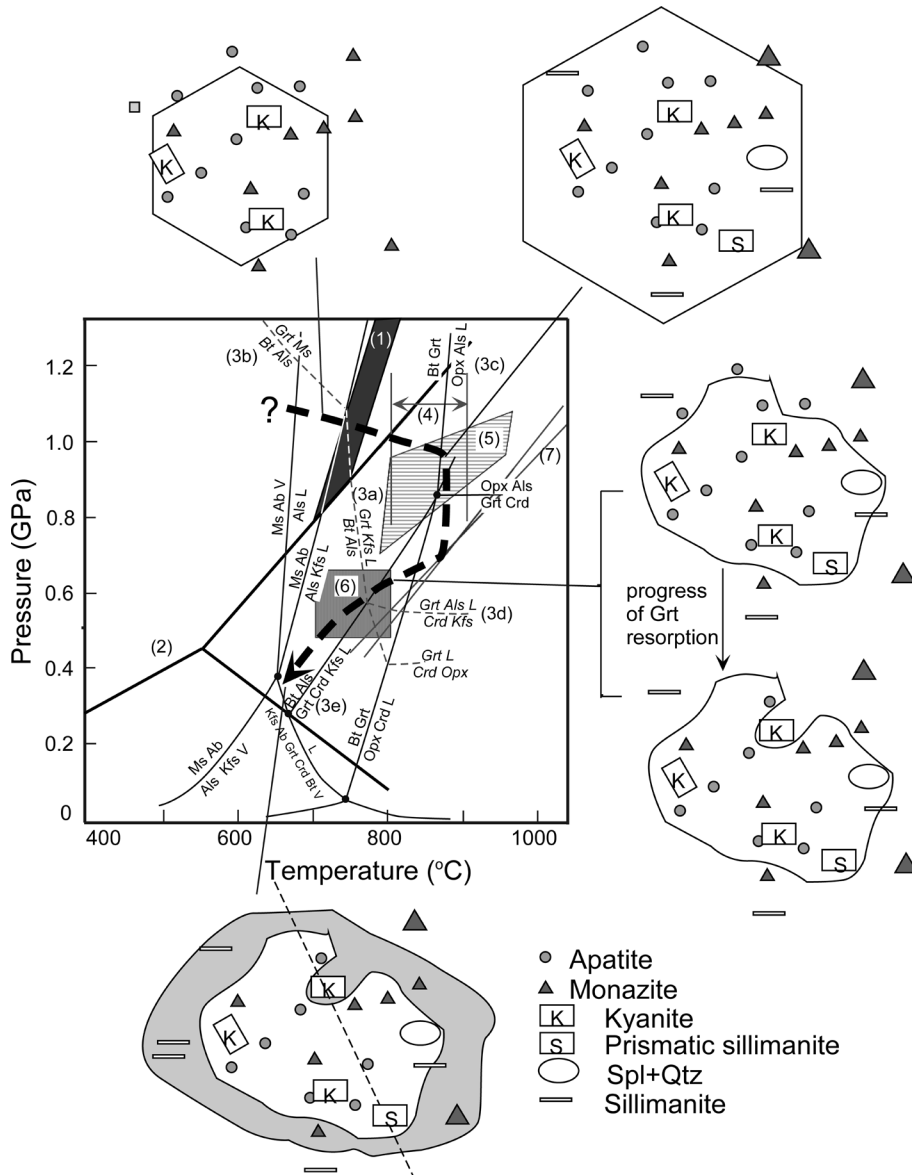
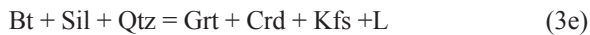


Figure 8. Illustration of the relationship between the *P-T* path and the garnet growth/resorption stages constrained by this study.



back reaction of reaction (3a) probably resorbed the garnet. Resorption of the phosphorus-poor garnet core occurred at this stage (Fig. 8). The variation of the aluminosilicate species included in the outermost core part of the garnet (Figs. 3–7) would have resulted from the difference in the extent of garnet core resorption. The decrease in pressure and temperature accompanied by garnet resorption continued until the *P-T* condition reached the vapor saturated solidus. Although the reaction line is not shown in Figure 2, the decrease in $P(\text{H}_2\text{O})$ possibly stabilized a reaction like:



to crystallize garnet at the vapor saturated solidus (Grant, 1985). The sillimanite-bearing rim of the garnet has to grow after gahnitic spinel + quartz formation, and no continuous reaction can grow garnet after the attainment of gahnitic spinel + quartz coexistence until the *P-T* path encounters the vapor saturated solidus. Therefore, it is quite likely that the $P(\text{H}_2\text{O})$ was low in the garnet-sillimanite gneiss when it finally crystallized at the vapor saturated solidus and the garnet rim including sillimanite needles was formed there. The phosphorus-rich rim probably formed at this stage (Fig. 8).

Possible origin of phosphorus-rich “island” in garnet core

The possible formation mechanism of “islands” in the

garnets shown in Figures 3 and 7 is discussed in this section, using the stepwise zoning of phosphorus as a contemporaneous surface. The “island” part could be a restitic garnet older than most garnet parts. Although this is possible, it cannot be proved or disproved conclusively at the present stage, and thus, it is not discussed here.

Another option is that the “island” part grew simultaneously with the phosphorus-rich garnet rim, as the phosphorus concentration in the “island” and the rim is quite similar (Figs. 3 and 7). In other words, this idea assumes that the phosphorus-rich “island” is the overgrown part after resorption and the phosphorus-rich garnet rim is three dimensionally connected with the “island.” One observation that might contradict this possibility is the occurrence of kyanite as an inclusion in the “island.” It is known from metamorphic zone mapping studies that prismatic kyanite tends to metastably survive in the sillimanite stability field without transforming to sillimanite, and new sillimanite needles nucleate elsewhere instead (e.g., Nagel et al., 2002). Therefore, it is likely that kyanite crystal in the “island” was once exposed to the rock-matrix when the garnet was resorped, and it survived metastably to be re-included in the phosphorus-rich rim of the garnet that overgrew the resorped core (Fig. 8). The distance of the kyanite from the resorption/recrystallization boundary is small, and this supports the hypothesis that kyanite in the “island” was only shortly exposed to the matrix environment to escape from its transformation to sillimanite.

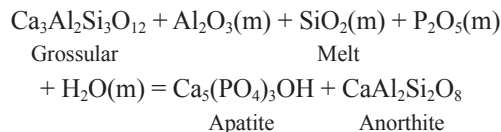
The outline of the intergrowth of muscovite + quartz (+ chlorite) included in the garnet “island” shown in Figure 7 is faceted. Chlorite is developed only between the garnet and the muscovite + quartz intergrowth, and probably a secondary product. If the “island” formation (garnet rim crystallization) occurred at the vapor saturated solidus, this would imply that melt crystallization occurred in the muscovite + quartz stability field. The presence of these types of “islands” in the midst of the garnet porphyroblasts requires further study.

Systematic change of phosphate inclusion assemblage and correlation with phosphorus zoning in garnet

In the Skallevikshalsen sample, the phosphate assemblage changes from apatite + monazite in the garnet core to monazite alone in the garnet rim, as described above. It is important to note that this change is accompanied by the discontinuous change in the phosphorus concentration in the garnet. The discontinuous increase in the phosphorus concentration in the garnet rim is often observed in high-temperature metamorphic rocks accompanying partial melting, and the correlation with the phosphate assem-

blage included in the garnet, as reported in this study, has actually been observed worldwide (Hiroi and Ellis, 1994; Hiroi, 1997; Hiroi et al., 1997; Yang and Rivers, 2002; Kawakami and Motoyoshi, 2004; Kawakami et al., 2008). However, the generalization of the phosphorus zoning correlated with the change in phosphate assemblage included in garnet cannot be easily carried out at the present stage because of the lack of the detailed case studies on this problem.

Yang and Rivers (2002) found that the garnet that coexists with apatite has smooth phosphorus zoning, and the phosphorus-content in garnet decreased systematically as the metamorphic grade increased from the garnet zone to the migmatite zone in Gagnon terrane, western Labrador. They considered that this systematic variation in phosphorus abundance with metamorphic grade and the smooth phosphorus zoning with no breaks imply that the activity of the phosphorus component in garnet was buffered by phase equilibria involving apatite and silicates (Yang and Rivers, 2002). Based on the similarity of phosphorus content in the studied garnet with that in other localities where similar peak metamorphic temperatures and different pressures are estimated, Yang and Rivers (2002) concluded that the phosphorus zoning of garnet that coexisted with apatite was mainly controlled by the change in temperature rather than that in pressure. The example of Yang and Rivers (2002) is mainly a subsolidus one. In the melt-bearing system, on the other hand, London et al. (1999) argue that silicate-phosphate equilibria are sufficiently numerous and diverse that the phosphorus content of magmas should normally be buffered by crystal-melt reactions. In the case of the garnet-sillimanite gneiss from Skallevikshalsen, partial melting would have occurred at the garnet-core formation stage (Fig. 2), and the presence of apatite and monazite inclusions in the garnet core suggests that phosphates might have buffered the phosphorus content of the melt through the reaction with silicates. For the melt to be saturated in apatite, because the solubility of the apatite is the activity product of all of its components, $[aCa]^5[aP]^3[aOH]$ has to be above the apatite saturation value. Consequently, the phosphorus content of the melt at saturation in any one of the crystalline phases will vary with the activities of other components (London et al., 1999) such as aCa . The addition of Ca (e.g., anorthite) will reduce the phosphorus content of the melt required to maintain apatite saturation (Wolf and London, 1994; London et al., 1999). Therefore, a reaction such as the one that follows might be important for the buffer of phosphorus content in the melt and other phases (four phases in the $CaO-Al_2O_3-SiO_2-P_2O_5$ system), where (m) denotes the component in the melt.



Other phosphorus-bearing phases like K-feldspar may also play an important role in buffering the phosphorus content in the melt and other phases. The silicate-phosphate equilibria are numerous and diverse (London et al., 1999), and therefore, it is difficult to specify the buffering reaction that actually worked in the Skallevikshalsen sample. However, Yang and Rivers (2002) showed that the phosphorus-content of garnet would be a function of temperature under the coexistence of apatite. Therefore, it is likely that the oscillatory-like zoning of phosphorus content in the garnet rim of the Skallevikshalsen sample (Fig. 7c) is the result of apatite disappearance when the garnet rim grew. That is, the oscillatory-like zoning of phosphorus content at the garnet rim (Fig. 7c) implies that phosphorus content was not buffered at the garnet rim growth stage.

The disappearance of apatite was probably caused by an increase in the melt formed through the biotite-consuming melting reactions such as reaction (3a) in the course of prograde metamorphism. This is possible if we accept the low whole-rock phosphorus-content of the garnet-sillimanite gneiss (Kawakami and Motoyoshi, 2004) to be an original characteristic of the protolith, because with such a characteristic, the partial melt formed in the garnet-sillimanite gneiss could become undersaturated in apatite under relatively low degree of partial melting and all the apatite can be consumed to finally form apatite-undersaturated melt. On the other hand, if we consider that the low whole-rock phosphorus-content represents the result of significant extraction of phosphorus-bearing melt from the originally phosphorus-rich garnet-sillimanite gneiss (e.g., Yoshimura et al., 2004), the disappearance of apatite by an increase in the melt remains possible, although the degree of melting has to be high.

On the crystallization of the partial melt, the crystallization of plagioclase probably lowered *a*Ca in the melt and hindered the crystallization of apatite (London et al., 1999). This is probably why the garnet rim of the Skallevikshalsen sample does not include apatite. It is likely that monazite did not play an important role in buffering the phosphorus content in the Skallevikshalsen sample.

ACKNOWLEDGMENTS

We would like to thank Dr. D. Dunkley, Ms. A. Nakamura, Prof. Y. Hiroi, and members of the JARE geology group for their fruitful discussions, especially through the

“Nishi-Higashi” seminars and NIPR symposiums. We would also like to thank Dr. M. Inui, Prof. M. Enami, and an anonymous reviewer for their constructive reviews and Prof. T. Hirajima for the editorial efforts. We thank Dr. K. Miyazaki for assistance with the X-ray mapping at AIST. This study was financially supported by the Kyoto University grant for young scientists, a grant from NIPR (general collaborative research program No. 19-15), and Grant-in-Aid for Young Scientists (B) (19740326) from JSPS to TK.

REFERENCES

- Chernoff, C.B. and Carlson, W.D. (1999) Trace element zoning as a record of chemical disequilibrium during garnet growth. *Geology*, 27, 555-558.
- Dunkley, D.J. (2007) Isotopic zonation in zircon as a recorder of progressive metamorphism. *Goldschmidt Conference Abstracts 2007*, A244.
- Grant, J.A. (1985) Phase equilibria in low-pressure partial melting of pelitic rocks. *American Journal of Science*, 285, 409-435.
- Hiroi, Y. (1997) Investigation into partial melting of rocks by means of metamorphic petrology. *Journal of Geography*, 106, 707-713 (in Japanese with English abstract).
- Hiroi, Y., Shiraishi, K., Nakai, Y., Kano, T. and Yoshikura, S. (1983a) Geology and petrology of Prince Olav Coast, East Antarctica. In *Antarctic Earth Science* (Oliver, R.L., James, P.R. and Jago, J.B. Eds.). Australian Academy of Science, Canberra, 32-35.
- Hiroi, Y., Shiraishi, K., Yanai, K. and Kizaki, K. (1983b) Aluminum silicates in the Prince Olav and Soya Coasts, East Antarctica. *Memoirs of National Institute for Polar Research, Special Issue*, 28, 115-131.
- Hiroi, Y., Shiraishi, K., Motoyoshi, Y., Kanisawa, S., Yanai, K. and Kizaki, K. (1986) Mode of occurrence, bulk chemical compositions, and mineral textures of ultramafic rocks in the Lützow-Holm Complex, East Antarctica. *Memoirs of National Institute for Polar Research, Special Issue*, 43, 62-84.
- Hiroi, Y., Shiraishi, K. and Motoyoshi, Y. (1991) Late Proterozoic paired metamorphic complexes in East Antarctica, with special reference to the tectonic significance of ultramafic rocks. In *Geological Evolution of Antarctica* (Thomson, M.R.A., Crame, J.A. and Thomson, J.W. Eds.). Cambridge University Press, Cambridge, 83-87.
- Hiroi, Y. and Ellis, D.J. (1994) The use of garnet porphyroblasts in highly deformed pelitic rocks to infer the former presence of partial melting. *Eos (Transactions, American Geophysical Union)*, 75, 364.
- Hiroi, Y., Ogo, Y. and Namba, K. (1994) Evidence for prograde metamorphic evolution of Sri Lanakan pelitic granulites, and implications for the development of continental crust. *Pre-cambrian Research*, 66, 245-263.
- Hiroi, Y., Seneviratne, L.K., Motoyoshi, Y., Ellis, D.J. and Kondo, Y. (1995) Compositional zoning of garnet in pelitic granulite from Sri Lanka: Four major elements (Fe, Mg, Mn, Ca). *The Journal of the Geological Society of Japan*, 101, VII-VIII.
- Hiroi, Y., Motoyoshi, Y., Ellis, D.J., Shiraishi, K. and Kondo, Y. (1997) The significance of phosphorus zonation in garnet from high grade pelitic rocks: A new indicator of partial melt-

- ing. In *The Antarctic Region* (Ricci, C.A. Ed.). Geological Evolution and Processes, Terra Antarctica Publication, Siena, 73–77.
- Ikeda, T. (2004) Garnet-biotite thermometry of a pelitic gneiss from the Lützow-Holm Complex in Skallen, East Antarctica: constraints on retrograde metamorphism. *Polar Geoscience*, 17, 45–57.
- Ishikawa, M., Motoyoshi, Y., Fraser, G.L. and Kawasaki, T. (1994) Structural evolution of Rundvågshetta region, Lützow-Holm Bay, East Antarctica. *Proceedings of the NIPR Symposium on Antarctic Geosciences*, 7, 69–89.
- Kawasaki, T., Ishikawa, M. and Motoyoshi, Y. (1993) A preliminary report on cordierite-bearing assemblages from Rundvågshetta region, Lützow-Holm Bay, East Antarctica. *Proceedings of the NIPR Symposium on Antarctic Geosciences*, 6, 47–56.
- Kawakami, T. and Ikeda, T. (2004) Timing of ductile deformation and peak metamorphism in Skallevikshalsen, Lützow-Holm Complex, East Antarctica. *Polar Geoscience*, 17, 1–11.
- Kawakami, T. and Motoyoshi, Y. (2004) Timing of attainment of spinel + quartz coexistence in garnet-sillimanite leucogneiss from Skallevikshalsen, Lützow-Holm Complex, East Antarctica. *Journal of Mineralogical and Petrological Sciences*, 99, 311–319.
- Kawakami, T., Ellis, D.J. and Christy, A.G. (2006) Sulfide evolution in high-temperature to ultrahigh-temperature metamorphic rocks from Lützow-Holm Complex, East Antarctica. *Lithos*, 92, 431–446.
- Kawakami, T., Grew, E.S., Motoyoshi, Y., Shearer, C.K., Ikeda, T., Burger, P.V. and Kusachi, I. (2008) Kornerupine *sensu stricto* associated with mafic and ultramafic rocks in the Lützow-Holm Complex at Akarui Point, East Antarctica: What is the source of boron? *Geological Society, London, Special Publications*, 308, 351–375.
- Kelsey, D.E., Clark, C. and Hand, M. (2008) Thermobarometric modelling of zircon and monazite growth in melt-bearing systems: examples using model metapelitic and metapsammitic granulites. *Journal of Metamorphic Geology*, 26, 199–212.
- London, D. (1997) Estimating abundances of volatile and other mobile components in evolved silicic melts through mineral-melt equilibria. *Journal of Petrology*, 38, 1691–1706.
- London, D., Wolf, M. B., Morgan, G. B. VI. and Gallego Garrido, M. (1999) Experimental silicate-phosphate equilibria in peraluminous granitic magmas, with a case study of the Albuquerque batholith at Tres Arroyos, Badajoz, Spain. *Journal of Petrology*, 40, 215–240.
- Motoyoshi, Y. (1986) Prograde and progressive metamorphism of the granulite facies Lützow-Holm Bay region, East Antarctica. pp. 238, D. Sc. thesis, Hokkaido University.
- Motoyoshi, Y. and Ishikawa, M. (1997) Metamorphic and structural evolution of granulites from Rundvågshetta, Lützow-Holm Bay, East Antarctica. In *The Antarctic Region* (Ricci, C.A. Ed.). Geological Evolution and Processes, Terra Antarctica Publication, Siena, 65–72.
- Nagel, T., de Capitani, C. and Frey, M. (2002) Isograds and *P-T* evolution in the eastern Lepontine Alps (Graubünden, Switzerland). *Journal of Metamorphic Geology*, 20, 309–320.
- Pattison, D.R.M. (1992) Stability of andalusite and sillimanite and the Al_2SiO_5 triple point: constraints from the Ballachulish aureole, Scotland. *Journal of Geology*, 100, 423–446.
- Satish-Kumar, M. and Wada, H. (2000) Carbon isotopic equilibrium between calcite and graphite in Skallen Marbles, East Antarctica: Evidence for preservation of peak metamorphic temperatures. *Chemical Geology*, 166, 173–182.
- Satish-Kumar, M., Hermann, J., Tsunogae, T. and Osanai, Y. (2006) Carbonation of Cl-rich scapolite boudins in Skallen, East Antarctica: evidence for changing fluid condition in the continental crust. *Journal of Metamorphic Geology*, 24, 241–261.
- Satish-Kumar, M., Hokada, T., Kawakami, T. and Dunkley, D. J. (2008) Geosciences research in East Antarctica (0°E–60°E): present status and future perspectives. *Geological Society, London, Special Publications*, 308, 1–20.
- Shiraishi, K., Hiroi, Y., Ellis, D.J., Fanning, C.M., Motoyoshi, Y. and Nakai, Y. (1992) The first report of a Cambrian orogenic belt in East Antarctica – An ion microprobe study of the Lützow-Holm Complex. In *Recent Progress in Antarctic Earth Science* (Yoshida, Y., Kaminuma, K. and Shiraishi, K. Eds.). Terra Scientific Publishing Company, Tokyo, 67–73.
- Shiraishi, K., Ellis, D.J., Hiroi, Y., Fanning, C.M., Motoyoshi, Y. and Nakai, Y. (1994) Cambrian orogenic belt in East Antarctica and Sri Lanka: Implications for Gondwana Assembly. *Journal of Geology*, 102, 47–65.
- Shiraishi, K., Hokada, T., Fanning, C.M., Misawa, K. and Motoyoshi, Y. (2003) Timing of thermal events in the Dronning Maud Land, East Antarctica. *Polar Geoscience*, 16, 76–99.
- Spear, F.S. and Kohn, M.J. (1996) Trace element zoning in garnet as a monitor of dehydration melting in pelites. *Geology*, 24, 1099–1102.
- Spear, F.S., Kohn, M.J. and Cheney, J.T. (1999) *P-T* paths from anatectic pelites. *Contributions to Mineralogy and Petrology*, 134, 17–32.
- Spear, F.S. and Pyle, J.M. (2002) Apatite, monazite, and xenotime in metamorphic rocks. *Reviews in Mineralogy and Geochemistry*, 48, 293–335.
- Wolf, M.B. and London, D. (1994) Apatite dissolution into peraluminous haplogranitic melts: An experimental study of solubilities and mechanisms. *Geochimica et Cosmochimica Acta*, 58, 4127–4145.
- Yang, P. and Rivers, T. (2002) The origin of Mn and Y annuli in garnet and the thermal dependence of P in garnet and Y in apatite in calc-pelite and pelite, Gagnon terrane, western Labrador. *Geological Materials Research*, v.4, n.1.
- Yoshida, M., Yoshida, Y., Ando, H., Ishikawa, T. and Tatsumi, T. (1976) Explanatory text of geological map of Skallen, Antarctica. Antarctic geological map series, Sheet 9, Skallen. pp. 16, National Institute of Polar Research.
- Yoshimura, Y., Motoyoshi, Y., Miyamoto, T., Grew, E.S., Carson, C.J. and Dunkley, D.J. (2004) High-grade metamorphic rocks from Skallevikshalsen in the Lützow-Holm Complex, East Antarctica: metamorphic conditions and possibility of partial melting. *Polar Geoscience*, 17, 57–87.
- Yoshimura, Y., Motoyoshi, Y. and Miyamoto, T. (2008) Sapphirine + quartz association in garnet: Implication for ultrahigh-temperature metamorphism in Rundvågshetta, Lützow-Holm Complex, East Antarctica. *Geological Society, London, Special Publications*, 308, 377–390.

Manuscript received May 1, 2008

Manuscript accepted January 8, 2010

Published online March 27, 2010

Manuscript handled by Takao Hirajima